Beyond Six Feet: A Guideline to Limit Indoor Airborne Transmission of COVID-19

Martin Z. Bazant[1,2*] and John W. M. Bush[2]

[1]*Department of Chemical Engineering*

[2]*Department of Mathematics, Massachusetts Institute of Technology, Cambridge, MA 02139, USA*

The revival of the world's economy is being predicated on the Six-Foot Rule, a guideline that offers little protection from pathogen-bearing droplets sufficiently small to be continuously mixed through an indoor space. The importance of indoor, airborne transmission of COVID-19 is now widely recognized; nevertheless, no quantitative measures have been proposed to protect against it. In this article, we build upon models of airborne disease transmission in order to derive a safety guideline that would impose a precise upper bound on the "cumulative exposure time", the product of the number of occupants and their time in an enclosed space. We demonstrate the manner in which this bound depends on the ventilation rate and dimensions of the room; the breathing rate, respiratory activity and face-mask use of its occupants; and the infectiousness of the respiratory aerosols, a disease-specific parameter that we estimate from available data. Case studies are presented, implications for contact tracing considered, and appropriate caveats enumerated.

Coronavirus disease 2019 (COVID-19) is an infectious pneumonia that appeared in Wuhan, Hubei Province, China in December 2019 and has since caused a global pandemic [1,2]. The

pathogen responsible for COVID-19, severe-acute-respiratory-syndrome coronavirus 2 (SARS-CoV-2), is known to be transported by respiratory droplets exhaled by an infected person [3–7]. There are thought to be three primary routes of human-to-human transmission of COVID-19, large drop transmission from the mouth of an infected person to the mouth, nose or eyes of the recipient, physical contact with droplets deposited on surfaces and subsequent transfer to the recipient's respiratory mucosae, and inhalation of the microdroplets and microparticles ejected by an infected person and held aloft by ambient air currents [6,8]. We subsequently refer to these three modes of transmission as, respectively, 'large-drop', 'contact' and 'airborne' transmission, while noting that the distinction between large-drop and airborne transmission is somewhat nebulous given the continuum of sizes of emitted droplets [9]. We here build upon the existing theoretical framework for describing airborne disease transmission [10–13] in order to characterize the evolution of the concentration of pathogen-laden droplets in a well-mixed room, and the associated risk of infection to its occupants.

The Six-Foot Rule is a social-distancing recommendation by the U.S. Centers for Disease Control and Transmission, based on the assumption that the primary vector of pathogen transmission is the large drops ejected from the most vigorous exhalation events, coughing and sneezing [5,14]. Indeed, high-speed visualization of such events reveals that six feet corresponds roughly to the maximum range of the largest, millimeter-scale drops [15]. Compliance to the Six-Foot Rule will thus substantially reduce the risk of such large-drop transmission. However, there is growing evidence that airborne transmission associated with relatively small, micron-scale droplets plays a significant, if not dominant, role in the spread of COVID-19 [4,5,7,14,16–18], particularly in the

so-called "super-spreading events" [19–21], which invariably occur indoors [22]. For example, at the 2.5-hour-long Skagit Valley Chorale choir practice that took place in Washington State on March 10, some 53 of 61 attendees were infected, presumably not all of them within 6 feet of the initially infected individual [19]. Moreover, a recent analysis over 7000 cases in China outside Hubei province found that all clusters of three or more transmissions occurred indoors, involving over 1200 cases, while only a single outbreak of two cases occurred outdoors [23].

The theoretical model developed herein informs the risk of transmission from the inhalation of small, micron-scale droplets that may remain suspended for extended periods within closed, well-mixed indoor spaces, thus potentially leading to airborne transmission. When people cough, sneeze, sing, speak or breathe, they expel an array of liquid droplets formed by the shear-induced destabilization of the mucosal linings of the lungs and respiratory tract [8,24]. When the person is infectious, these droplets are potentially pathogen bearing, and represent the principle vector of disease transmission. The range of the exhaled pathogens is determined by the radii of the carrier droplets, which typically lie in the range of 0.5μm - 1 mm. While the majority are submicron, the drop size distribution depends on the form of exhalation events [9]. For normal breathing, the drop radii vary between 0.25 and 2.5 μm, with a peak at 0.75 μm [9,17,25]. Relatively large drops are more prevalent in the case of more violent expiratory events such as coughing and sneezing [15,26]. The ultimate fate of the droplets is determined by their size and the air flows they encounter [27,28]. Exhalation events are accompanied by a time-dependent gas-phase flow emitted from the mouth that may be roughly characterized in terms of either continuous turbulent jets or discrete puffs [15,25,29]. The precise form of the gas flow depends on the nature of the exhalation event, specifically the

time-dependence of the flux of air expelled. Coughs and sneezes result in violent, episodic puff releases [15], while peaking and singing result in a puff train that may be well approximated as a continuous turbulent jet [25,29]. Eventually, the small droplets settle out of this turbulent gas flow. In the presence of a quiescent ambient, they then settle to the floor; however, in the well-mixed ambient typical of a ventilated space, sufficiently small drops may be suspended by the ambient airflow and mixed throughout the room until being removed by the ventilation outflow or inhaled.

Existing theoretical models of airborne disease transmission in closed, well-mixed spaces are based on the seminal work of Wells [30] and Riley *et al.* [31], and have been applied to describe the spread of airborne pathogens including tuberculosis, measles, influenza, H1N1, coronavirus (SARS-CoV) [10–13,32,33] and most recently, the novel coronavirus (SARS-CoV-2) [18,19]. These models are all based on the premise that the space of interest is well mixed; thus, the pathogen is distributed uniformly throughout. In such well-mixed spaces, one is no safer from airborne pathogens at 60 feet than 6 feet. The Wells-Riley model [11,12] highlights the role of the room's ventilation outflow rate Q on the rate of infection, showing that the transmission rate is inversely proportional to Q, a trend supported by data on the spreading of airborne respiratory diseases on college campuses [34]. The additional effects of viral deactivation, sedimentation dynamics and the polydispersity of the suspended droplets were introduced by Stilianakis & Drossinos [13] and recently applied to COVID-19 [18]. The equations describing pathogen transport in well-mixed, closed spaces are thus well established. We here use them to derive a quantitative guideline for mitigating airborne transmission. Incorporating data characterizing the physical properties of expiratory ejecta allows us to quantify the heightened risk of various activities, including speaking and singing, and

the benefits of wearing face masks.

We begin by describing the dynamics of airborne pathogen in a well-mixed room, on the basis of which we deduce an estimate for the rate of inhalation of pathogen by its occupants. We proceed by deducing the associated infection rate from a single infected individual to a susceptible person. We illustrate how the model's epidemiological parameter, a measure of the infectiousness of COVID-19, may be estimated from available epidemiological data, including transmission rates in a number of spreading events, expiratory drop size distributions [9] and the infectivity of such droplets bearing SARS-CoV-2 [3]. Our estimates for this parameter are shown to align with those recently reported [18], but call for refinement through consideration of more such field data. Most importantly, our study yields a guideline for mitigating airborne transmission via limitation of indoor occupancy and exposure time, and allows for a quantitative assessment of risk in various settings.

The Well-Mixed Room

We first characterize the evolution of the pathogen concentration in a well-mixed room. We do so by adapting standard methods developed in chemical engineering to describe the 'continuously stirred tank reactor' [35]. We assume that the droplet-borne pathogen remains airborne for some time before either being extracted by the room's ventilation system, inhaled or sedimenting out. The fate of ejected droplets is determined by the relative magnitudes of two speeds, the settling speed of the drop in quiescent air, v_s, and the ambient air circulation speed within the room, v_a. Drops

of radius $r \leq 100\mu$m and density ρ_d descend through air of density ρ_a and dynamic viscosity μ_a at the Stokes settling speed $v_s(r) = \frac{2}{9}\Delta\rho g r^2/\mu_{air}$, prescribed by the balance between gravity and viscous drag, where g is the gravitational acceleration and $\Delta\rho = \rho_d - \rho_a$. We consider a well-mixed room of area A, depth H and volume $V = AH$ with ventilation outflow rate Q (as distinct from air recirculation rate) and air change rate (ACH) $\lambda_a = Q/V$. Equating the characteristic times of droplet settling, H/v_s, and removal, V/Q, indicates a critical drop radius $r_c = \sqrt{9\lambda_a H\mu_a/(2g\Delta\rho)}$ above which drops generally sediment out, and below which they remain largely suspended within the room prior to removal by ventilation outflow. We here define airborne transmission as that associated with droplets with radius $r < r_c$. The relevant physical picture, of particles settling from a well-mixed environment, is commonly invoked in the context of both stirred aerosols [36] and sedimentation in geophysics [37]. The additional effects of ventilation, particle dispersity and pathogen deactivation relevant in the context of airborne disease transmission were considered by Stiliankakis & Drossinos [13] and Buonanno et al. [18], whose models will be built upon here.

It is noteworthy that, even in the absence of forced ventilation, there will generally be some mixing in an enclosed space: natural ventilation will lead to flows through windows or doors, and occupants will create additional air flow through their motion and respiration. Ventilation standards for American homes (ASHRAE 2016) recommend a minimal air exchange rate of $\lambda_a = 0.35$/h, a value comparable to the average of 0.34/h reported for Chinese apartments, including winter in Wuhan during the initial outbreak [38]. Even with such minimal ventilation rates, for a room of height $H = 2.1$m there is an associated critical drop size of radius $r_c = 1.3\mu$m. The 'airborne' droplets of interest here, those of radius $r < r_c$, thus constitute a significant fraction of those emitted in

most respiratory events [9,17,25]. Moreover, a recent experimental study of the dependence of droplet size on the infectiousness of SARS-CoV-2 virions [3] concluded that droplets with $r > 2\mu$m are less infectious, an inference that would underscore the importance of airborne transmission.

We consider a polydisperse suspension of exhaled droplets characterized by the number density $n_d(r)$ (per volume of air) of drops of radius r and volume $V_d(r) = \frac{4}{3}\pi r^3$. The drop size distribution $n_d(r)$ is known to vary strongly with respiratory activity and various physiological factors [9,18]. The drops contain a microscopic pathogen concentration $c_v(r)$, a drop-size-dependent probability of finding individual virions [3], usually taken to be that in the sputum (RNA copies per mL) [18]. The virions become deactivated (non-infectious) at a rate $\lambda_v(r)$ that may in principle depend on droplet radius or humidity [39]. However, since this dependence is not yet well characterized experimentally for SARS-CoV-2 in airborne droplets, we treat the deactivation rate as a constant bounded by existing estimates [19], $\lambda_v = 0 - 0.63$/h. We note that deactivation rates may be enhanced by ultraviolet radiation (UV-C) [40], chemical disinfectants (*e.g.* H_2O_2, O_3) [41], or high-efficiency particulate air (HEPA) filtration [42].

We seek to characterize the concentration $C(r,t)$ of pathogen (per volume of air) transported by drops of radius r. We assume that each infectious individual exhales pathogen-laden droplets of radius r at a constant rate $P(r) = Q_b n_d(r) V_d(r) p_m(r) c_v(r)$ (number/time), where Q_b is the breathing flow rate (exhaled volume per time). We introduce a mask penetration factor, $0 < p_m(r) < 1$, that accounts for the ability of masks to filter droplets [43,44]. The concentration, $C(r,t)$,

of pathogen suspended within drops of radius r per infector then evolves according to

$$V\left(\frac{\partial C}{\partial t}+\lambda_v C\right)=I(t)P(r)-QC-v_s(r)AC. \tag{1}$$

where $v_s(r)$ is the particle settling speed. Owing to the dependence of the settling speed on particle radius, the population of each drop size evolves, according to equation (1), at different rates. Two limiting cases of Eq.1 are of interest. For the case of $\lambda_v = v_s = 0$, drops of infinitesimal size that do not deactivate, it reduces to the Wells-Riley model [30,31]. For the case of $\lambda_v = P = Q = 0$, a non-reacting suspension with no ventilation, it corresponds to established models of sedimentation from a well-mixed ambient [36,37]. For the sake of notational simplicity, we define a size-dependent sedimentation rate $\lambda_s(r) = v_s(r)/H = \lambda_a(r/r_c)^2$ as the inverse of the time taken for a drop of radius r to sediment from ceiling to floor in a quiescent room.

When one infected individual enters a room at time $t = 0$, the radius-resolved pathogen concentration increases as, $C(r,t) = C_s(r)\left(1-e^{-\lambda_c(r)t}\right)$, relaxing to a steady value, $C_s(r) = P(r)/(\lambda_c(r)V)$, at a rate, $\lambda_c(r) = \lambda_a + \lambda_s(r) + \lambda_v$. Note that both the equilibrium concentration and the timescale to approach it are decreased by the combined effects of ventilation, particle settling and deactivation [39]. Owing to the dependence of this adjustment process on the drop size, one may understand it as a dynamic sifting process wherein larger droplets settle out and reach their equilibrium concentration relatively quickly. However, we note that this adjustment time, λ_c^{-1}, depends only weakly on drop size, varying from $V/(2Q)$ for the largest airborne drops (with radius r_c) to V/Q for infinitesimal drops. The sedimentation rate of the 'airborne' droplets of radius $r \leq r_c$ is thus bounded above by the air exchange rate, $\lambda_s(r) \leq \lambda_a$. The exhaled drop-size distribution depends strongly on respiratory activity [9,18,25,45]; thus, so too must the radius-resolved

concentration of airborne pathogen. The predicted dependence on respiratory activity [9] of the steady-state volume fraction of airborne droplets, $\phi_s(r) = C_s(r)/c_v(r)$ is illustrated in Fig. 1.

We define the airborne disease transmission rate, $\beta_a(t)$, as the mean number of transmissions per time between a given pair of infectious and susceptible individuals. One expects $\beta_a(t)$ to be proportional to the quantity of pathogen exhaled by the infected person, and to that inhaled by the susceptible person. Gammaitoni and Nucci [10] defined the airborne transmission rate as $\beta_a(t) = Q_b c_i C_s(t)$ for the case of a population evolving according to the Wells-Riley model and inhaling a monodisperse suspension. Here, c_i is the viral infectivity, the parameter that connects fluid physics to epidemiology, specifically the concentration of suspended pathogen to the infection rate. We note its relation to the notion of "infection quanta" in the epidemiological literature [30]: c_i is the infection quanta per pathogen. The value of c_i has been inferred to lie in the range 0.01-0.1 for SARS-CoV [46] and conjectured to be comparable for SARS-CoV-2 [18].

For the polydisperse suspension of interest here, we define the airborne transmission rate as

$$\beta_a(t) = Q_b \int_0^\infty C(r,t) p_m(r) c_i(r) dr, \tag{2}$$

thereby accounting for the protective properties of masks, and allowing for the possibility that the infectivity $c_i(r)$ depends on droplet size. Different droplet sizes may emerge from, and penetrate into, different regions of the respiratory tract, and so have different $c_i(r)$; moreover, virions on relatively small droplets may diffuse to surfaces more rapidly and so exchange with bodily fluids more effectively. Such a size dependence in infectivity, $c_i(r)$, is also consistent with the recent experiments of Santarpia *et al.* [3], who reported that replication of SARS-CoV-2 is more apparent

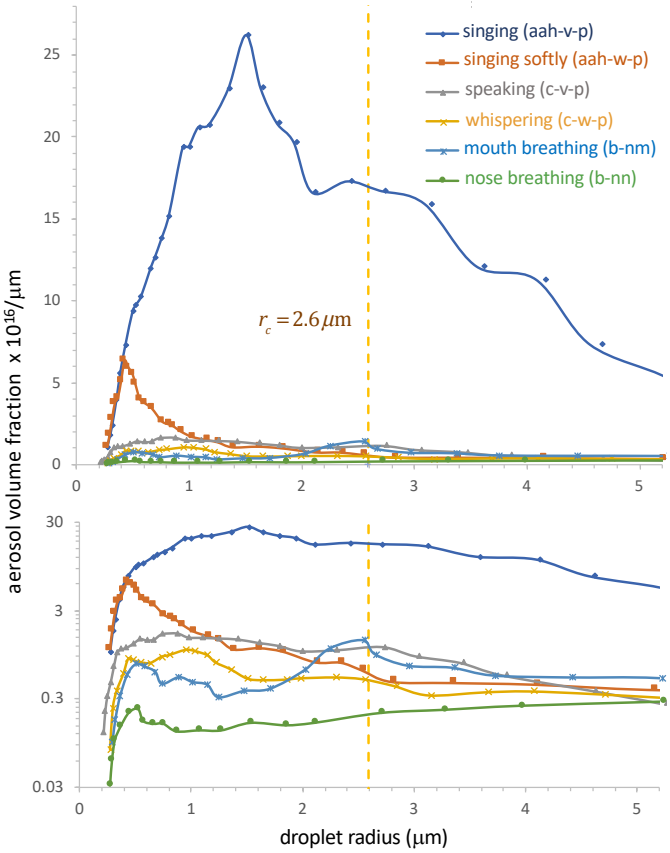

Figure 1: Model predictions for the steady-state, droplet-radius-resolved aerosol volume fraction, $\phi_s(r)$, produced by a single infectious person in a well-mixed room. The model accounts for the effects of ventilation, pathogen deactivation and droplet settling for several different types of respiration in the absence of facemasks ($p_m = 1$). The ambient conditions are taken to be those of the Skagit Valley Chorale super-spreading incident[19,21] ($H = 4.5$m, $A = 180$m^2, $\lambda_a = 0.65$h^{-1}, $\lambda_v = 0.3$h^{-1}, $r_c = 2.6\mu$m). The expiratory droplet size distributions are computed from the data of Morawska *et al.*[9] (Fig. 3) for aerosol concentration per log-diameter, using $n_d(r) = (dC/d\log D)/(r\ln 10)$. The breathing flow rate is assumed to be 0.5 m^3/h for nose and mouth breathing, 0.75 m^3/h for whispering and speaking, and 1.0 m^3/h for singing.

in droplets with radii $r < 2.05\mu$m, despite a nearly uniform viral load, $c_v(r)$, across all drop sizes.

Indoor Safety Guideline

The reproduction number of an epidemic, $\mathcal{R}_0$, is defined as the mean number of transmissions per infected individual. Provided $\mathcal{R}_0 < 1$, a disease will not spread at the *population* level [47]. Estimates of $\mathcal{R}_0$ for COVID-19 have been used to compare its rate of spread in different regions and its dependence on different control strategies. [48–50] We here define an analogous reproductive number for indoor, airborne transmission, $\mathcal{R}_{in}(\tau)$, as the expected number of transmissions in a room of total occupancy N over a time τ from a single infected person entering at $t = 0$.

Our safety guideline sets a small tolerance ϵ for the indoor reproductive number, defined as

$$\mathcal{R}_{in}(\tau) = (N-1)\int_0^\tau \beta_a(t)\,dt < \epsilon \tag{3}$$

One may interpret $\mathcal{R}_{in}(\tau)$ as the probability of the first transmission, a probability that can be expressed as the sum of $N-1$ independent transmission probabilities to each susceptible person in a well mixed room. As shown in the Supplementary Information, this guideline follows from standard epidemiological models, including the Wells-Riley model, in the $\epsilon \ll 1$ limit, but has broader generality. The exact transient safety bound, Eq. (3), appropriate for the time-dependent situation soon after the entrance of the infected index case, is evaluated in Methods.

We here focus on a simpler and more conservative guideline that follows for long times relative to the air residence time, $\tau \gg \lambda_a^{-1}$ (which may vary from minutes to hours), when the

airborne pathogen has attained its equilibrium concentration $C(r,t) \to C_s(r)$. In this equilibrium case, the transmission rate (2) becomes constant:

$$\overline{\beta}_a = \frac{Q_b^2 p_m^2}{V} \int_0^\infty \frac{n_q(r)}{\lambda_c(r)} dr = \frac{Q_b^2 p_m^2}{V} \frac{C_q}{\lambda_c(\overline{r})} = p_m^2 f_d \lambda_q \tag{4}$$

where, for the sake of simplicity, we assume constant mask filtration p_m over the entire range of aerosol drop sizes. We define the microscopic concentration of infection quanta per liquid volume as $n_q(r) = n_d(r) V_d(r) c_v(r) c_i(r)$, and the concentration of infection quanta or "infectiousness" of exhaled air, $C_q = \int_0^\infty n_q(r) dr$. The latter is the key disease-specific parameter in our model, which can also be expressed as the rate of quanta emission, $\lambda_q = Q_b C_q$, by an infected person. The second equality in Eq. (4) defines the effective radius $\overline{r}$ of the settling drops (see Eq. (11) in Methods). The third equality defines the dilution factor, $f_d = Q_b/(\lambda_c(\overline{r})V)$, the ratio of the concentration of infection quanta in the well-mixed room to that in the unfiltered breath of an infected person. As we shall see in what follows, this dilution factor provides a valuable diagnostic in assessing the relative risk of various forms of exposure.

We thus arrive at a simple guideline, appropriate for steady-state situations, that bounds the *cumulative exposure time* (CET):

$$(N-1)\tau < \epsilon \frac{(\lambda_a + \lambda_v)V + \overline{v}_s A}{Q_b^2 p_m^2 C_q}. \tag{5}$$

By noting that the sedimentation rate is effectively bounded by the air exchange rate, $\lambda_s(r) < \lambda_a$, and neglecting pathogen deactivation, we deduce from Eq. (5) a more conservative CET bound,

$$N\tau < \epsilon \frac{\lambda_a V}{Q_b^2 p_m^2 C_q}, \tag{6}$$

the interpretation of which is immediately clear. To minimize risk of infection, one should avoid spending extended periods in highly populated areas. One is safer in rooms with large volume and high ventilation rates. One is at greater risk in rooms where people are exerting themselves in such a way as to increase their respiration rate and pathogen output, for example by exercising, singing or shouting. Since the rate of inhalation of contagion depends on the volume flux of both the exhalation of the infected individual and the inhalation of the susceptible person, the risk of infection increases as Q_b^2. Likewise, masks worn by both infected and susceptible persons will reduce the risk of transmission by a factor p_m^2, a dramatic effect given that $p_m \leq 0.1$ for typical masks [43,44].

Application to COVID-19

The only poorly constrained quantity in our guideline is the epidemiological parameter, C_q, the concentration of exhaled infection quanta by an infectious individual. While C_q is expected to vary widely between different populations [51–53] and among individuals during progression of the disease [54,55], we proceed with a view to making rough estimates for C_q for different respiratory activities on the basis of existing epidemiological data. We do so with the hope that such an attempt will motivate the acquisition of more such data, and so to improved estimates for C_q in various settings.

An inference of $C_q = 970$ quanta/m^3 was made by Miller *et al.* [19] in their recent analysis of the Skagit Valley Chorale super-spreading incident [21], on the basis of the assumption that the

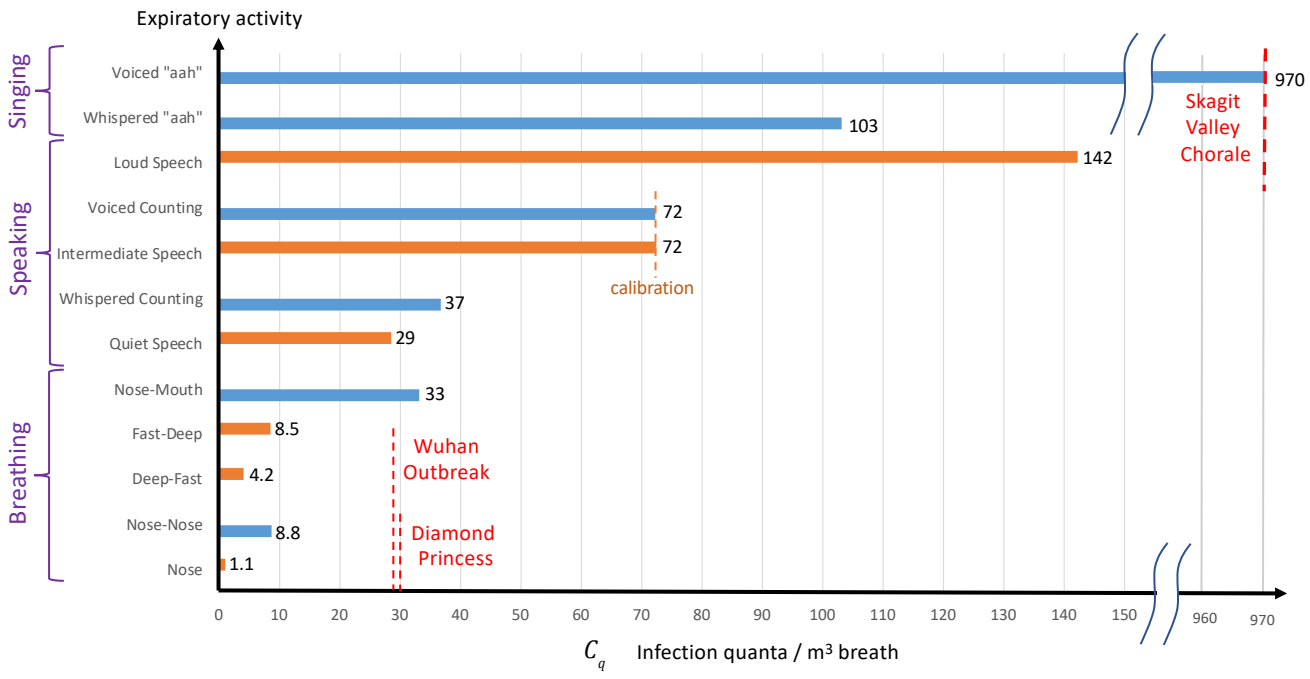

Figure 2: Estimates of the COVID-19 "infectiousness" of exhaled air, C_q, defined as the concentration of infection quanta in the breath of an infected person, for various respiratory activities. Values are deduced from the drop-size distributions reported by Morawska *et al.* [9] (blue bars) and Asadi *et al.* [45] (orange bars). The only value reported in the epidemiology literature, $C_q = 970$ quanta/m^3, was estimated [19] for the Skagit Valley Chorale super-spreading event [21]. This value is rescaled by the predicted infectious aerosol volume fractions, $\phi_1(r) = \int_0^{r_c} \phi_s(r)\, dr$, obtained by integrating the steady-state size distributions reported in Fig. 1 for different expiratory activities [9]. Aerosol volume fractions calculated for various respiratory activities from Fig. 5 of Asadi et al. [45] are rescaled so that the value $C_q = 72$ quanta/m^3 for "intermediate" speaking matches that inferred from Morawska *et al.*'s [9] for "voiced counting". Estimates of C_q for the outbreak during the quarantine period of the Diamond Princess and the initial outbreak in Wuhan City are also shown (see Supplementary Information for details).

transmission was described in terms of the Wells-Riley model [10,11,18,31]. This inference for C_q is roughly consistent with studies of other related viral diseases. For example, Liao *et al.* [32] estimated $C_q = 28$ quanta/m^3 from the rate of indoor spreading of SARS-CoV, in a hospital and an elementary school. Estimates of C_q for H1N1 influenza fall in the range $15 - 128$ quanta/m^3 [33]. For SARS-CoV-2, Buonanno *et al.* [18] estimate a C_q range of 10.5-1030 quanta/m^3, on the basis of the estimated infectivity $c_i = 0.01 - 0.1$ of SARS-CoV [46] and the reported viral loads in sputum [54–56], and note that the precise value depends strongly on the infected person's respiratory activity. Notably, their range spans the high value inferred for the Skagit Valley Chorale [19], and all of our inferences to follow.

We proceed by estimating quanta emission rates C_q for different forms of respiration. First, we solve Eq. (1) to obtain the steady-state radius-resolved droplet volume fraction $\phi_s(r)$ for various hypothetical expiratory activities in the room of the Skagit Valley Chorale, using the drop size distributions of Morawska *et al.* [9]. Our results are shown in Fig. 1. Integrating each curve up to the critical radius r_c, we then obtain an activity-dependent volume fraction of infectious airborne droplets $\phi_1 = \int_0^{r_c} \phi_s(r)\, dr$ in the choir room (see Supplementary Information). Finally, we assume that the inferred value, $C_q = 970$, for the super-spreading incident [19] resulted from the expiratory activity most resembling singing (voiced "aahs" with pauses for recovery [9]), and deduce values of C_q for other forms of respiration by rescaling with the appropriate ϕ_1 values. Our predictions for the dependence of C_q on respiratory activity are shown in Fig. 2. For validation, we also show estimates for C_q based on the recent measurements of activity-dependent aerosol concentrations reported by Asadi *et al.* [25,45]. Specifically, we calculated the aerosol volume fractions from the

reported drop-size distributions (from Fig. 5 of Ref.[45]) for a different set of expiratory activities that included various breathing patterns and speaking aloud at different volumes. We then used these volume fractions to rescale the value $C_q = 72$ quanta/m^3 for speaking at intermediate volume [45], which we chose to match the value inferred for the most similar respiratory activity considered by Morawska *et al.* [9], specifically voiced counting with pauses [9]. Notably, the quanta concentrations so inferred, C_q, are consistent across the full range of activities, from nasal breathing at rest (1-10 q/m^3) to oral breathing and whispering (5-40 q/m^3), to loud speaking and singing (100-1000 q/m^3).

Our inferences for C_q are also roughly consistent with physiological measurements of viral RNA in the bodily fluids of COVID-19 patients. Specifically, our estimate of $C_q = 72$ quanta/m^3 for voiced counting [9] and intermediate-volume speech [45] with integrated aerosol volume fractions $\phi_1 = 0.36$ and 0.11 (μm/cm)^3 corresponds, respectively, to microscopic concentrations of $c_q = c_i c_v = 2 \times 10^8$ and 7×10^8 quanta/mL (see Supplementary Information). Viral loads, c_v, in sputum tend to peak in the range $10^8 - 10^{11}$ RNA copies/mL [54–56], while much lower values have been reported for other bodily fluids [54,55,57]. Virus shedding in the pharynx remains high during the first week of symptoms and reaches 7×10^8 RNA copies per throat swab [54] (typically 1-3 mL). Since viral loads are 20-50% greater in sputum than in throat swabs [55], the most infectious aerosols are likely to contain $c_v \approx 10^9$ RNA copies/mL. Using this value and the mean infectivity $c_i = 2\%$ reported for SARS-CoV [46], Buonanno *et al* [18] inferred $c_q = 2 \times 10^7$ q/mL for SARS-CoV-2, an order of magnitude below our estimates obtained directly from spreading data for COVID-19. The inference that SARS-CoV-2 is ten times more infectious than SARS-CoV, with $c_i > 10\%$, is consistent with the fact that only the former achieved pandemic status.

Our findings are consistent with emerging physiological [3] and epidemiological [5,14,17,22] evidence that SARS-CoV-2 is present and extremely infectious in respiratory aerosols and that indoor airborne transmission may be the primary driver of the COVID-19 pandemic [4,16]. Further support for this hypothesis is provided by crudely applying our indoor transmission model to the initial outbreak of COVID-19 in Wuhan [2,48]. We assume that spreading occurred predominantly in family apartments, as is consistent with the inference that 80% of transmission clusters arose in homes [23]. We may then tentatively equate the average reproduction number estimated for the Wuhan outbreak [48], $\mathcal{R}_0 = 3.3$, with the indoor reproduction number, $\mathcal{R}_{in}(\tau)$. We use $\tau = 5.5$ days as the exposure time, assuming that it corresponds to mean time before the onset of symptoms and patient isolation. We consider the mean household size of 3.03 persons in a typical apartment with area 30 m^2/person and a winter bedroom ventilation rate of 0.34 ACH [38], and assume that $\lambda_v = 0.3$/h and $\bar{r} = 2\mu$m. We thus infer that $C_q = 30$ quanta/m^3, which is consistent with the inference of Fig. 2 for normal breathing. As detailed in Supplementary Information, a comparable value can be inferred from a similar analysis of spreading of COVID-19 aboard the quarantined Diamond Princess cruise ship [20], although that the extent to which the Diamond Princess can be adequately described in terms of a closed, well-mixed space remains the subject of some debate.

In summary, our inferences of C_q from a diverse set of indoor spreading events and from independent physiological data are sufficiently self-consistent to indicate that the values reported in Fig. 2 may prove to be sufficient to apply the safety guideline in a quantitative fashion. Our hope is that our attempts to infer C_q will motivate the collection of more such data from spreading events, which might then be used to refine our necessarily crude initial estimates.

Case studies and contact tracing

We proceed by illustrating the value of our guideline in estimating the maximum occupancy or exposure time in two settings of particular interest, the classroom and an elder care facility. Considering our inferences from the data and the existing literature, it would appear reasonable to illustrate our guideline for COVID-19 with the choice, $C_q = 30$ quanta/m^3, bearing in mind that this value varies strongly with different demographics and respiratory activity levels [18]. We thus assume that in both settings considered, occupants are engaged in relatively mild respiratory activities consistent with quiet speech or rest. In assessing critical cumulative exposure times for given populations, we stress that the tolerance ϵ is a parameter that should be chosen judiciously according to the vulnerability of the population, which varies dramatically with age and pre-existing conditions [51–53].

We first apply our guideline to a typical classroom in the United States, designed for the standard occupancy of 19 students and their teacher (see Fig. 3(a)). The importance of adequate ventilation and mask use is made clear by our guideline. For normal occupancy and without masks, the expected time for the first transmission after an infected individual enters the classroom is 2.3 hours for natural ventilation and 18 hours with mechanical ventilation, according to the transient bound (12) with $\epsilon = 1$. These time limits are multiplied by ϵ/p_m^2 in our safety guideline, and so would reach 23 to 180 hours with low-quality masks ($p_m = 0.1$) and a tolerance of $\epsilon = 0.1$. Assuming six hours of indoor time per day, a school group wearing masks could thus meet for several days between the testing and subsequent removal of any newly infected individuals. With

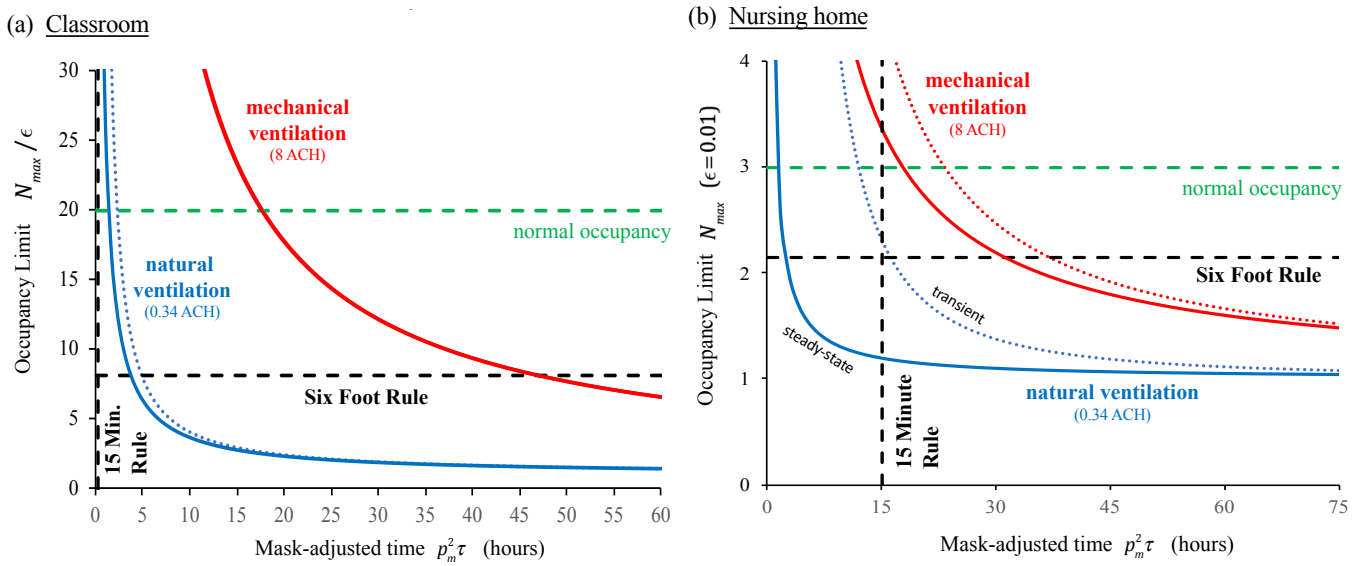

Figure 3: The COVID-19 indoor safety guideline would limit the *cumulative exposure time* to lie beneath the curves shown. Evidently, the Six-Foot Rule becomes inadequate after a critical time, and the 15-Minute Rule above a critical occupancy. (a) Risk-adjusted occupancy, N_{max}/ϵ, versus mask-adjusted time, $p_m^2\tau$, spent indoors with an infected person. We choose typical values appropriate for a school classroom: 20 persons share a room with an area of 900 square feet and a ceiling height of 12 feet ($A = 83.6$ m^2, $V = 301$ m^3). (b) Nursing home shared room with a maximum occupancy of three ($A = 22.3$ m^2, $V = 53.5$ m^3), and a risk tolerance of $\epsilon = 0.01$ chosen to reflect the vulnerability of the community. In both cases, curves deduced from the pseudo-steady formula, Eq. (5), are shown for both natural ventilation ($\lambda_a = 0.34$/h; blue curve) and mechanical ventilation ($\lambda_a = 8.0$/h; red curve). The transient formula (Eq.12 in Methods) is shown with dotted curves. System parameters are $C_q = 30$ quanta/m^3, $\lambda_v = 0.3$/h, $Q_b = 0.5$ m^3/h, $\overline{r} = 0.5\mu$m, $\overline{v}_s = 0.108$ m/h. We stress that in (a), the maximum occupancy is normalized by the risk tolerance ϵ, the occupancy time by the squared mask penetration factor, p_m^2; thus, the deduction of concrete numbers for maximum occupancy N_{max} for a given time, or maximum occupancy time for a given N, requires an appropriate scale factor.

enhanced ventilation and judicious mask use, this time limit could be extended to several weeks, and so exceed the recovery time for COVID-19. We stress, however, that these predictions assume a "quiet classroom", where resting respiration ($C_q = 30$) is the norm. Extended periods of physical activity, collective speech, or singing would lower the time limit by an order of magnitude (Fig. 2).

Our analysis sounds the alarm for elderly homes and long-term care facilities, which account for a large fraction of COVID-19 hospitalizations and deaths [51–53]. In nursing homes in New York City, law requires a maximum occupancy of three and recommends a mininum area of 80 square feet per person. In Fig. 3(b), we plot the guideline for a tolerance of $\epsilon = 0.01$ transmission probability, chosen to reflect the vulnerability of the community. Once again, the effect of ventilation is striking. For natural ventilation (0.34 ACH), the Six Foot Rule fails after only 3 minutes under quasi-steady conditions, or after 17 minutes for the transient response to the arrival of an infected person, in which case the 15 Minute Rule is only marginally safe. With mechanical ventilation (at 8 ACH) in steady state, three occupants could safely remain in the room for no more than 18 minutes. This example provides insight into the devastating toll of the COVID-19 pandemic on the elderly [51,53]. Furthermore, it underscores the need to minimize the sharing of indoor space, maintain adequate, once-through ventilation, and encourage the use of face masks.

In both examples, the benefit of face masks is immediately apparent, since the CET limit is enhanced by a factor p_m^{-2}, the inverse *square* of the mask penetration factor. Standard disposable surgical masks are characterized by $p_m = 1 - 5\%$ [43], and so allow the cumulative exposure time to be extended by 400-10000 times. Even improvised cloth face coverings achieve $p_m =$

$10 - 20\%$ [44], and so would extend recommended exposure times by a factor of 25-100. Our inference of the efficacy of face masks in mitigating airborne transmission is roughly consistent with studies showing the benefits of mask use on COVID-19 transmission at the scale of both cities and countries [16,49].

Finally, we illustrate the value of our guideline in contact tracing [50], specifically, in prescribing the scope of the testing of people with whom an infected index case has had close contact. The CDC presently defines a COVID-19 "close contact" as any encounter in which an individual is within 6 feet of an infected person for at least 15 minutes. Figure 3 makes clear that this definition may grossly underestimate the number of individuals exposed to a substantial risk of airborne infection in indoor spaces. Our study suggests that whenever our CET bound (5) is violated during an indoor event involving the index case, one transmission is likely, with probability ϵ. When the tolerance ϵ exceeds a critical value, *all* occupants of the room should be considered close contacts and so warrant testing. For relatively short exposures ($\lambda_a \tau \ll 1$) initiated when the index case enters the room, the transient bound (12) should be considered.

For instructions on how to apply our guideline to other situations, we refer the interested reader to the spreadsheet provided in the Supplementary Information. There, by specifying a given room geometry, ventilation rate and respiratory activity, one may deduce the maximum cumulative exposure time in a particular indoor setting, and so define precisely what constitutes an exposure in that setting.

Beyond the Well-Mixed Room

The model developed herein describes the risk of small respiratory drops ($r < r_c$) in the case where the entirety of the room is well mixed. There are undoubtedly circumstances where there are substantial spatial and temporal variations of the pathogen concentration from the mean [7,28]. For example, it is presumably the spatial variations from well-mixedness that result in the inhomogeneous infection patterns reported for a number of well-documented transmission events in closed spaces, including a COVID outbreak in a Chinese restaurant [4], and SARS outbreaks on airliners [58]. In the vicinity of an infected person, the turbulent respiratory jet or plume will have a pathogen concentration that is substantially higher than the ambient [15,29]. Chen *et al.* [28] referred to infection via respiratory plumes as 'short-range airborne transmission', and demonstrated that it poses a substantially greater risk than large-drop transmission.

On the basis of the relatively simple geometric form of turbulent jet and puff flows, one may make estimates of the form of the mixing that respiratory outflows induce, the spatial distribution of their pathogen concentration and so the resulting risk they pose to the room's occupants. For the case of the turbulent jet associated with relatively continuous speaking or breathing, turbulent entrainment of the ambient air leads to the jet radius $r = \alpha x$ increasing linearly with distance x from the source, where $\alpha \sim 0.1 - 0.15$ is the typical jet entrainment coefficient [15,28,29]. The conservation of momentum flux $M = \pi \rho_a r^2 v^2$ then indicates that the jet speed decreases with distance from the source according to $v(x) = M^{1/2}/(\pi \rho_a \alpha x)$. Concurrently, turbulent entrainment results in the pathogen concentration within the jet decreasing according to $C_j(x)/C_0 = A_m^{1/2}/(\alpha x)$,

where $A_m \sim 2\text{cm}^2$ denotes the cross-sectional area of the mouth and $C_0 = C_q/c_v$ is the exhaled pathogen concentration. Abkarian *et al.* [29] thus deduce that for the respiratory jet generated by typical speaking, the concentration of pathogen is diminished to approximately 3% of its initial value at a distance of 2 meters.

In a well-mixed room, the mean concentration of pathogen produced by a single infected person is $f_d C_0$. For example, in the large, poorly ventilated room of the Skagit Valley Choir practice, we compute a dilution factor, $f_d = Q_b/(\lambda_c(\bar{r})V)$ of approximately 0.001. We note that since $\lambda_c(r) > \lambda_a = Q/V$, the dilution factor satisfies the bound, $f_d \leq Q_b/Q$. For typical rooms and air exchange rates, f_d lies in the range of $0.0001 - 0.01$. With the dilution factor of the well-mixed room and the dilution rate of respiratory jets, we may now assess the relative risk to a susceptible person of a close encounter (either episodic or prolonged) with an infected individual's respiratory jet, and an exposure associated with sharing a room with an infected person for an extended period of time. Since the infected jet concentration $C_j(x)$ decreases with distance from its source, one may assess its pathogen concentration relative to that of the well-mixed room, $C_j(x)/(f_d C_0) = A_m^{1/2}/(\alpha f_d x)$. There is thus a critical distance, $A_m^{1/2}/(\alpha f_d)$ beyond which the pathogen concentration in the jet is reduced to that of the ambient. This distance exceeds 10m for f_d in the aforementioned range and so is typically much greater than the characteristic room dimension. Thus, in the absence of masks, respiratory jets may pose a substantially greater risk than the well-mixed ambient.

We first consider a worst-case, close-contact scenario in which a person directly ingests a

lung full of air exhaled by an infected person. An equivalent amount of pathogen would be inhaled from the ambient by anyone within the room after a time $\tau = V_b/(Q_b f_d)$, where $V_b \approx 500$ mL is the volume per breath. For the geometry of the Skagit choir room, for which $f_d = 0.001$, the critical time beyond which airborne transmission is a greater risk than this worst-case close encounter with a respiratory plume is $\tau = 1.0$ hour. We next consider the worst-case scenario governed by the 6-foot rule, in which a susceptible person is directly in the path of an infected turbulent jet at a distance of 6 feet, over which the jet is diluted by factor of 3% [29]. The associated concentration in the jet is still roughly 30 times higher than the steady-state concentration in the well-mixed ambient (when $f_d = 0.001$), and so would result in a commensurate amplification of the transmission probability. We note that our guideline could thus be adopted to safeguard against the risk of respiratory jets in a socially-distanced environment by reducing ϵ by a factor of $C(6ft)/(f_d C_0)$, which is 3 - 300 for f_d in the range of 0.0001 - 001. We note that the latter worst-case scenario describes a static situation where a susceptible individual is seated directly in the respiratory plume of an infected individual, as may arise in a classroom or airplane [58]. More generally, with a circulating population in an indoor setting, one would expect to encounter an infected respiratory plume only for some small fraction of the time, consideration of which would allow for a less conservative choice of ϵ.

Finally, we note that the use of face-masks will have a marked effect on respiratory jets, with the fluxes of both exhaled pathogen and momentum being reduced substantially at their source. Indeed, Chen *et al.* [28] note that when masks are worn, the primary respiratory flow may be described in terms of a rising thermal plume, which is of significantly less risk to neighbours. With a

population of individuals wearing face masks, the risk posed by respiratory jets will thus be largely eliminated, while that of the well-mixed ambient will remain.

Discussion and Caveats

We have focused here primarily on airborne transmission, for which infection arises through inhalation of a critical quantity of airborne pathogen, and neglected the roles of both contact and large-drop transmission [6]. However, we note that the approach taken, coupling the droplet dynamics to the transmission dynamics, allows for a more complete description. For example, consideration of conservation of pathogen allows one to calculate the rate of pathogen sedimentation and associated surface contamination, consideration of which would allow for quantitative models of contact transmission and so inform cleaning protocols. A more comprehensive theory of the dynamics of disease transmission in enclosed spaces will be presented elsewhere.

Typical values for the parameters arising in our model are listed in Table 1 of the Supplementary Information. Respiration rates Q_b have been measured to be $\sim 0.5\text{m}^3$/hr for normal breathing, and may increase by a factor of 3 for more strenuous activities [18]. Other parameters, including room geometry (V, A and $H = V/A$) and ventilation rate will be room dependent. The most poorly constrained parameter appearing in our guideline is C_q, the concentration of pathogen in the breath of an infected person. However, using the value inferred for the Skagit Valley Chorale incident [19], the best characterized super-spreading event, and rescaling using reported drop-size distributions [9,17,25] has allowed us to estimate C_q for several respiratory activities, as listed in Fig-

ure 3. Further comparison with new inferences based on other super-spreading effects would allow for refinement of our estimates of C_q. As we expect such inferences to depend strongly on several factors, including the mean age of the population [52], one might also infer, in principle, how the infectivity depends on these factors. We thus appeal to the public health and epidemiology communities to document the physical conditions enumerated in Table 1 of the Supplementary Information for more indoor spreading events.

Adherence to the Six-Foot Rule would limit large-drop transmission, and to our guideline (5) would limit airborne transmission. We have also shown how the sizeable variations in pathogen concentration associated with near-field respiratory flows arising (in a population not wearing face-masks) might be taken into account, leading to a guideline that would bound both the distance between occupants and the cumulative exposure time. Circumstances may also arise, owing to the absence or deficiency of the air-conditioning or to irregularities in the room geometry and air circulation, where a room is only partially mixed. In the context of reducing COVID transmission in indoor spaces, such considerations need be made on a room-by-room basis. Nevertheless, the criterion (5) represents a minimal requirement for safety from airborne infection in well-mixed, indoor spaces.

We note further that we have neglected the influence of ambient humidity, which one expects to determine the rates of droplet shrinkage via evaporation or growth via condensation, and so influence the drop size distribution and ambient infectivity, C_q [8,9,28]. Moreover, we note that we have assumed that the global dynamics may be described in terms of a mean infectivity and

susceptibility, while recent evidence suggests that there may be significant age-related variability in both [51–53]. We emphasize that our inferences of C_q are all rooted in that inferred from the Skagit Valley Chorale super-spreading event [19], where the median age was 69 [21]; thus, the values reported in Fig. 2 are likely to represent conservative overestimates of C_q for younger, less vulnerable populations.

Our theoretical model of the well-mixed room was developed specifically to describe airborne transmission between a fixed number of individuals in a single well-mixed room. Nevertheless, we note that it is likely to inform a broader class of transmission events. For example, there are situations where forced ventilation mixes air between rooms, in which case the compound room becomes effectively a well-mixed space. Examples considered here are the outbreaks on the Diamond Princess and in apartments in Wuhan City (see Supplementary Information); others would include prisons. There are many other settings, including classrooms and factories, where people come and go, in which case, they interact intermittently with the space, with infected people exhaling into it, and susceptible inhaling from it, for limited periods. This class of problems is also informed by our model provided one considers the mean population dynamics, specifically, that N be identified as the mean number of occupants.

Finally, the guideline (5) depends on the tolerance ϵ, whose value in a particular setting should be set by the appropriate policy makers, informed by the latest epidemiological evidence. Nevertheless, this factor may be eliminated from consideration by using (6) to assess the *relative behavioral risk* posed to a particular individual by attending a specific event of duration τ with N

other participants. We thus define a risk index,

$$I_R = \frac{N\tau C_q Q_b^2 p_m^2}{\lambda_a V}, \tag{7}$$

that may be evaluated using appropriate C_q and Q_b values listed in Figure 3. One's risk increases linearly with the number of people in a room and duration of the event. Relative risk decreases for large, well ventilated rooms and increases when the room's occupants are exerting themselves or speaking loudly. While these results are intuitive, the approach taken here provides a physical framework for understanding them quantitatively. It also provides a quantitative measure of the relative risk of certain environments, for example, a well ventilated, sparsely occupied laboratory and a poorly ventilated, crowded, noisy bar. Along similar lines, the weighted average of (7), provides a quantitative assessment of one's risk of airborne infection over an extended period. It thus allows for a quantitative assessment of what constitutes an *exposure*, a valuable notion in defining the scope of contact tracing.

Above all, our study makes clear the inadequacy of the Six-Foot Rule in mitigating indoor airborne disease transmission, and offers a rational, physically-informed alternative for managing life in the time of COVID-19. If implemented, our safety guideline would impose a limit on the cumulative exposure time in indoor settings, violation of which constitutes an exposure for all of the room's occupants. The spreadsheet included in the Supplementary Information provides a simple means of evaluating this limit for any particular indoor setting. Finally, our study indicates how new data on indoor spreading events may lead to improved estimates of the infectiousness of the disease and so to quantitative refinements of our safety guideline.

Methods

Exact solution for the transient guideline The general safety guideline (3) can be written as, $\mathcal{R}_{in}(\tau) = (N-1)\langle\beta_a\rangle\tau$, in terms of the time-averaged airborne transmission rate, which can be broken into steady-state and transient terms:

$$\langle\beta_a\rangle(\tau) = \frac{1}{\tau}\int_0^\tau \beta_a(t)dt = \overline{\beta}_a - \Delta\beta_a(\tau) \tag{8}$$

$$\overline{\beta}_a = \frac{Q_b^2}{V}\int_0^\infty \frac{n_q(r)}{\lambda_c(r)}dr \tag{9}$$

$$\Delta\beta_a(\tau) = \frac{Q_b^2}{V\tau}\int_0^\infty \frac{n_q(r)}{\lambda_c(r)^2}\left(1-e^{-\lambda_c(r)\tau}\right)dr \tag{10}$$

where $n_q(r) = n_d(r)V_d(r)c_v(r)c_i(r)$ and $\lambda_c(r) = \lambda_a(1+(r/r_c)^2)+\lambda_v$. The steady-state term $\overline{\beta}_a$ can be expressed as Eq. (4), where the mean sedimentation speed $v_s(\overline{r})$ and mean suspended droplet size, $\overline{r}$, are defined by

$$\frac{v_s(\overline{r})}{\nu^2 v_a} = \left(\frac{\overline{r}}{\nu r_c}\right)^2 = \left(\frac{1}{C_q}\int_0^\infty \frac{n_q(r)dr}{1+(r/(\nu r_c))^2}\right)^{-1} - 1 \tag{11}$$

with $v_a = Q/A$ and $\nu = \sqrt{1+\lambda_v/\lambda_a}$, which gives most weight in the average to the suspended aerosol droplets with $r < r_c$.

For short exposures or poor ventilation, the transient correction can reduce the indoor reproductive number, resulting in a more permissive guideline. In the case of monodisperse droplets of size $r = \bar{r}$, the transient term can be approximated as, $\Delta\beta_a/\overline{\beta}_a = (1-e^{-\lambda_c\tau})/(\lambda_c\tau) \approx 1/(1+\lambda_c\tau)$. We may thus recast the general safety guideline in the form,

$$(N-1)\overline{\beta}\tau < \epsilon(1+(\lambda_c(r)\tau)^{-1}) \tag{12}$$

which reduces to the pseudo-steady criterion, $(N-1)\tau\overline{\beta} < \epsilon$ for exposure times long relative

to the concentration relaxation time, $\lambda_c(r)\tau \gg 1$. In the limit of short exposures, $\lambda_c(r)\tau \ll 1$, we obtain a refined safety guideline, $(N-1)(\overline{\beta}\tau)(\lambda_c(r)\tau) < \epsilon$, which is less strict because it reflects the leeway associated with the time taken for the build-up of the airborne pathogen following the arrival of an infected person. During this period, the safe exposure time scales as $\tau_{max} \sim \sqrt{(N-1)}$, and the CET bound diverges as $(N-1)\tau_{max} \sim \tau^{-1}$ in the limit $\tau \to 0$. This divergence simply reflects the fact that transmission will not occur if people do not spend sufficient time together.

Acknowledgements The authors would like to thank William Ristenpart and Sima Asadi for sharing experimental data and Lesley Bazant, Lydia Bourouiba, Daniel Cogswell and Mark Hampden-Smith for important references.

Competing Interests The authors declare that they have no competing financial interests.

Correspondence Correspondence and requests for materials should be addressed to M. Z. B. (email: bazant@mit.edu).

References

1. Chen, N. *et al.* Epidemiological and clinical characteristics of 99 cases of 2019 novel coronavirus pneumonia in Wuhan, China: a descriptive study. *The Lancet* **395**, 507–513 (2020).

2. Li, Q. *et al.* Early transmission dynamics in Wuhan, China, of novel coronavirus–infected pneumonia. *New England Journal of Medicine* **382**, 1199–1207 (2020).

3. Santarpia, J. L. *et al.* The infectious nature of patient-generated SARS-CoV-2 aerosol. *medRxiv preprint* (2020).

4. Morawska, L. & Milton, D. K. It is time to address airborne transmission of COVID-19. *Clinical Infectious Diseases* ciaa939 (2020).

5. Morawska, L. & Cao, J. Airborne transmission of SARS-CoV-2: The world should face the reality. *Environment International* **139**, 105730 (2020).

6. Mittal, R., Ni, R. & Seo, J.-H. The flow physics of COVID-19. *Journal of Fluid Mechanics* **894**, F2 (2020).

7. Jayaweera, M., Perera, H., Gunawardana, B. & Manatunge, J. Transmission of COVID-19 virus by droplets and aerosols: A critical review on the unresolved dichotomy. *Environ Res.* **188** (2020).

8. Morawksa, L. Droplet fate in indoor environments, or can we prevent the spread of infection? *Indoor Air* **16**, 335–347 (2006).

9. Morawska, L. *et al.* Size distribution and sites of origin of droplets expelled from the human respiratory tract during expiratory activities. *Journal of Aerosol Science* **40**, 256–269 (2009).

10. Gammaitoni, L. & Nucci, M. C. Using a mathematical model to evaluate the efficacy of TB control measures. *Emerging Infectious Diseases* **3**, 335 (1997).

11. Beggs, C., Noakes, C., Sleigh, P., Fletcher, L. & Siddiqi, K. The transmission of tuberculosis in confined spaces: an analytical review of alternative epidemiological models. *The international journal of tuberculosis and lung disease* **7**, 1015–1026 (2003).

12. Noakes, C., Beggs, C., Sleigh, P. & Kerr, K. Modelling the transmission of airborne infections in enclosed spaces. *Epidemiology & Infection* **134**, 1082–1091 (2006).

13. Stilianakis, N. I. & Drossinos, Y. Dynamics of infectious disease transmission by inhalable respiratory droplets. *Journal of the Royal Society Interface* **7**, 1355–1366 (2010).

14. Setti, L. *et al.* Airborne transmission route of COVID-19: Why 2 meters/6 feet of inter-personal distance could not be enough. *Int. J. Environ. Res. Public Health* **17**, 1–6 (2020).

15. Bourouiba, L., Dehandschoewercker, E. & Bush, J. W. M. Violent expiratory events: on coughing and sneezing. *Journal of Fluid Mechanics* **745**, 537–563 (2014).

16. Zhang, R., Li, Y., Zhang, A. L., Wang, Y. & Molina, M. J. Identifying airborne transmission as the dominant route for the spread of COVID-19. *Proc. Nat. Acad. Sci.* **117**, 14857–14863 (2020).

17. Asadi, S., Bouvier, N., Wexler, A. S. & Ristenpart, W. D. The coronavirus pandemic and aerosols: Does COVID-19 transmit via expiratory particles? *Aerosol Science and Technology* **54**, 635–638 (2020).

18. Buonanno, G., Stabile, L. & Morawska, L. Estimation of airborne viral emission: quanta emission rate of SARS-CoV-2 for infection risk assessment. *Environment International* **141**, 105794 (2020).

19. Miller, S. L. *et al.* Transmission of SARS-CoV-2 by inhalation of respiratory aerosol in the Skagit Valley Chorale superspreading event. *medRxiv preprint* (2020).

20. Moriarty, L. F. Public health responses to COVID-19 outbreaks on cruise ships worldwide, February–March 2020. *MMWR. Morbidity and Mortality Weekly Report* **69** (2020).

21. Hamner, L. High SARS-CoV-2 attack rate following exposure at a choir practice, Skagit County, Washington, March 2020. *MMWR. Morbidity and Mortality Weekly Report* **69** (2020).

22. Nishiura, H. *et al.* Closed environments facilitate secondary transmission of coronavirus disease 2019 (COVID-19). *medRxiv preprint* (2020).

23. Qian, H. *et al.* Indoor transmission of sars-cov-2. *medRxiv preprint* (2020).

24. Johnson, D. & Morawska, L. The mechanism of breath aerosol formation. *J. Aerosol Medicine and Pulmonary Drug Delivery* **22**, 229–237 (2009).

25. Asadi, S. *et al.* Aerosol emission and superemission during human speech increase with voice loudness. *Scientific Reports* **9**, 1–10 (2019).

26. Scharfman, B. E., Techet, A. H., Bush, J. W. M. & Bourouiba, L. Visualization of sneeze ejecta: steps of fluid fragmentation leading to respiratory droplets. *Experiments in Fluids* **57**, 24 (2016).

27. Gralton, J., Tovey, E., McLaws, M.-L. & Rawlinson, W. D. The role of particle size in aerosolised pathogen transmission: A review. *Journal of Infection* **62**, 1–13 (2011).

28. Chen, W., Zhang, N., Wei, J., Yen, H.-L. & Li, Y. Short-range airborne route dominates exposure of respiratory infection during close contact. *Building and Environment* 106859 (2020).

29. Abkarian, M., Mendez, S., Xue, N., Yang, F. & Stone, H. A. Puff trains in speaking produce long-range turbulent jet-like transport potentially relevant to asymptomatic spreading of viruses. *arXiv preprint arXiv:2006.10671* (2020).

30. Wells, W. F. *et al.* Airborne contagion and air hygiene. an ecological study of droplet infections. *Airborne Contagion and Air Hygiene. An Ecological Study of Droplet Infections.* (1955).

31. Riley, E. C., Murphy, G. & Riley, R. L. Airborne spread of measles in a suburban elementary school. *American Journal of Epidemiology* **107**, 421–432 (1978).

32. Liao, C.-M., Chang, C.-F. & Liang, H.-M. A probabilistic transmission dynamic model to assess indoor airborne infection risks. *Risk Analysis* **25**, 1097–1107 (2005).

33. Rudnick, S. & Milton, D. Risk of indoor airborne infection transmission estimated from carbon dioxide concentration. *Indoor air* **13**, 237–245 (2003).

34. Zhu, S. *et al.* Ventilation and laboratory confirmed acute respiratory infection (ari) rates in college residence halls in college park, maryland. *Environment international* **137**, 105537 (2020).

35. Davis, M. E. & Davis, R. J. *Fundamentals of Chemical Reaction Engineering* (Courier Corporation, 2012).

36. Corner, J. & Pendlebury, E. The coagulation and deposition of a stirred aerosol. *Proceedings of the Physical Society. Section B* **64**, 645 (1951).

37. Martin, D. & Nokes, R. Crystal settling in a vigorously converting magma chamber. *Nature* **332**, 534–536 (1988).

38. Hou, J. *et al.* Air change rates in urban Chinese bedrooms. *Indoor air* **29**, 828–839 (2019).

39. Yang, W. & Marr, L. C. Dynamics of airborne influenza a viruses indoors and dependence on humidity. *PLOS ONE* **6** (2011).

40. García de Abajo, F. J. *et al.* Back to normal: An old physics route to reduce sars-cov-2 transmission in indoor spaces. *ACS nano* **14**, 7704–7713 (2020).

41. Schwartz, A. *et al.* Decontamination and reuse of n95 respirators with hydrogen peroxide vapor to address worldwide personal protective equipment shortages during the sars-cov-2 (covid-19) pandemic. *Applied Biosafety* **25**, 67–70 (2020).

42. Mousavi, E. S., Pollitt, K. J. G., Sherman, J. & Martinello, R. A. Performance analysis of portable hepa filters and temporary plastic anterooms on the spread of surrogate coronavirus. *Building and Environment* 107186 (2020).

43. Oberg, T. & Brosseau, L. M. Surgical mask filter and fit performance. *American journal of infection control* **36**, 276–282 (2008).

44. Konda, A. *et al.* Aerosol filtration efficiency of common fabrics used in respiratory cloth masks. *ACS Nano* **14**, 6339–6347 (2020).

45. Asadi, S. *et al.* Effect of voicing and articulation manner on aerosol particle emission during human speech. *PloS one* **15**, e0227699 (2020).

46. Watanabe, T., Bartrand, T. A., Weir, M. H., Omura, T. & Haas, C. N. Development of a dose-response model for SARS coronavirus. *Risk Analysis* **30**, 1129–1138 (2010).

47. Kermack, W. O. & McKendrick, A. G. A contribution to the mathematical theory of epidemics. *Proc. Roy. Soc. London. Series A* **115**, 700–721 (1927).

48. Liu, Y., Gayle, A. A., Wilder-Smith, A. & Rocklöv, J. The reproductive number of COVID-19 is higher compared to SARS coronavirus. *Journal of Travel Medicine* **27**, 1–4 (2020).

49. Stutt, R. O. J. H., Retkute, R., Bradley, M., Gilligan, C. A. & Colvin, J. A modelling framework to assess the likely effectiveness of facemasks in combination with lock-down in managing the COVID-19 pandemic. *Proc. R. Soc. A.* **476**, 20200376 (2020).

50. Ferretti, L. *et al.* Quantifying SARS-CoV-2 transmission suggests epidemic control with digital contact tracing. *Science* **368** (2020).

51. Richardson, S. *et al.* Presenting characteristics, comorbidities, and outcomes among 5700 patients hospitalized with COVID-19 in the New York City area. *JAMA* **323**, 2052–2059 (2020).

52. Davies, N., Klepac, P., Liu, Y. *et al.* Age-dependent effects in the transmission and control of COVID-19 epidemics. *Nature Medicine* **898** (2020).

53. Garg, S. Hospitalization rates and characteristics of patients hospitalized with laboratory-confirmed coronavirus disease 2019: COVID-NET, 14 States, March 1–30, 2020. *MMWR. Morbidity and Mortality Weekly Report* **69** (2020).

54. Wölfel, R. *et al.* Virological assessment of hospitalized patients with covid-2019. *Nature* **581**, 465–469 (2020).

55. Pan, Y., Zhang, D., Yang, P., Poon, L. L. & Wang, Q. Viral load of SARS-CoV-2 in clinical samples. *The Lancet Infectious Diseases* **20**, 411–412 (2020).

56. To, K. K.-W. *et al.* Temporal profiles of viral load in posterior oropharyngeal saliva samples and serum antibody responses during infection by SARS-CoV-2: an observational cohort study. *The Lancet Infectious Diseases* **20**, 565–574 (2020).

57. Zheng, S. *et al.* Viral load dynamics and disease severity in patients infected with SARS-CoV-2 in Zhejiang province, China, January-March 2020: retrospective cohort study. *British Medical Journal* **369** (2020).

58. Olsen, S., Chang, H.-L. *et al.* Transmission of the severe acute respiratory syndrome on aircraft. *New England J. Medicine* **349**, 2146–2422 (2003).